Morphological Anisotropic Diffusion

C. Andrew Segall and Scott T. Acton
Oklahoma Imaging Laboratory
School of Electrical and Computer Engineering
Oklahoma State University
Stillwater, OK 74078

Abstract

*Current formulations of anisotropic diffusion are unable to prevent feature drift **and** smooth small regions. These deficiencies reduce the effectiveness of the diffusion operation in many image processing tasks, including segmentation, edge detection, compression, and multi-scale processing. This paper introduces a morphological diffusion coefficient capable of smoothing small objects while maintaining edge locality. Results are presented that demonstrate its efficacy in edge detection tasks.*

I. Introduction

The anisotropic diffusion equation provides a technique for selective image smoothing. Preserving contrast by incorporating region boundaries within the filtering operation, anisotropic diffusion adaptively filters a signal by encouraging intra-region smoothing while inhibiting inter-region interactions. Originally introduced as an alternative to traditional linear scale generating kernels [6], the design of this nonlinear process was motivated by the need to reduce the movement of edges.

While anisotropic diffusion does reduce feature drift, it does not guarantee the removal of small scale detail, and the existence of these small features introduces problems for a variety of signal processing applications, including filtering, sampling, and system stability. More recent expressions of anisotropic diffusion can smooth small regions, but reintroduce feature drift and edge movement.

In this paper, a realization of the anisotropic diffusion equation capable of smoothing small features while preserving edge locality is introduced. The paper is organized as follows: The second section provides background on the anisotropic diffusion equation and discusses previous coefficient realizations. Section III introduces a new diffusion coefficient based on morphological operators. Section IV reveals numerical and visual comparisons of the proposed coefficient and two standard diffusion approaches.

This material is based upon work supported by the U.S. Army Research Office under grant number DAAH04-95-1-0255.

II. Anisotropic Diffusion

It has been shown that the Gaussian filter can be implemented with the heat equation [5]. For a two dimensional image $\mathbf{I}$, this is expressed as

$$\frac{\partial \mathbf{I}}{\partial t} = \frac{\partial^2 \mathbf{I}}{\partial x^2} + \frac{\partial^2 \mathbf{I}}{\partial y^2}, \tag{1}$$

where the variance of the Gaussian kernel is proportional to the solution time, t.

In proposing a filter which removes the problem of feature drift, Perona and Malik introduced the nonlinear smoothing expression

$$\frac{\partial \mathbf{I}}{\partial t} = div[c\nabla \mathbf{I}], \tag{2}$$

where div is the divergence operator, $\nabla \mathbf{I}$ is the image gradient, and c is the diffusion coefficient [6]. Allowing the diffusion coefficient to vary with respect to the local image gradient produces anisotropic diffusion, and the success of the anisotropic diffusion approach is strongly tied to the method of computing the diffusion coefficient.

Original coefficient implementations were dependent solely on local gradient information. One suggestion was

$$c = e^{-\left(\frac{\|\nabla \mathbf{I}\|}{k}\right)^2}, \tag{3}$$

where c is the diffusion coefficient and k is a gradient threshold [6].

Basing the anisotropic diffusion coefficient completely on local gradients does create a filter capable of smoothing an image while maintaining edge locality;

0-8186-8183-7/97 $10.00 © 1997 IEEE

however, it is unable to remove small scale features with high contrast. This property makes anisotropic diffusion unsuitable for the removal of heavy-tailed noise and inappropriate as a sampling prefilter. Additionally, it results in a mathematically ill-posed process, as small changes in the original image produce large changes in the filtered result [9]. These problems may be overcome by computing the gradient across a larger region.

The first coefficient implementation capable of increasing the scale of the gradient was introduced by Catté *et al.* [2]. By smoothing the image used in the gradient calculation, the form

$$c = e^{-\left(\frac{\|\nabla(G_\sigma * \mathbf{I})\|}{k}\right)^2} \tag{4}$$

was introduced, where G_σ is a Gaussian weighted lowpass filter of standard deviation σ, $\mathbf{I}$ is the image, and k is the gradient threshold.

Prefiltering the gradient is an attractive and effective method for allowing the anisotropic diffusion process to remove small, high contrast regions. Unfortunately, while the problems inherent to the original anisotropic diffusion equation are reduced, the use of a linear filter reintroduces edge movement, defeating the primary motivation of the anisotropic diffusion process.

To develop a diffusion coefficient capable of smoothing small scale objects while minimizing feature drift, regions must be identified without removing important high frequency content. This criterion suggests the use of nonlinear filters, and the construction of a diffusion coefficient based on nonlinear morphological operators is discussed in the next section.

III. Morphological Anisotropic Diffusion

Morphological operators are able to produce image representations of increasing scale without eradicating edges. Approaching image processing from the vantage point of human perception, morphological operators simplify image data, preserving essential shape characteristics and eliminating irrelevancies [4]. These properties make them well suited for identifying small features and allowing the diffusion equation to smooth them. For an introduction to morphological filtering, see [8].

The choice of morphological filter type is crucial to the development of a new diffusion coefficient. Fundamental operators, such as erosion and dilation, are unsuitable as they induce edge movement. Simple combinations of these operators, such as opening and closing, reduce feature drift but introduce an intrinsic gray scale bias, removing only light or dark features.

The morphological close-open filter effectively identifies regions without removing high frequency information, without introducing edge drift, and without exhibiting gray scale bias. Substituting these nonlinear morphological operators for the linear filter in (4) results in a new diffusion coefficient

$$c = e^{-\left(\frac{\|\nabla((\mathbf{I}\bullet\mathbf{K})\circ\mathbf{K})\|}{k}\right)^2}, \tag{5}$$

where $\mathbf{I}$ is the original image, k is the gradient threshold, and $(\mathbf{I}\bullet\mathbf{K})\circ\mathbf{K}$ is the morphological close-open filter.

Applying morphological operators to the anisotropic diffusion coefficient allows the diffusion equation to smooth objects smaller than the structuring element, $\mathbf{K}$, while maintaining edge structure and location. In the next section, results are presented which compare the new diffusion coefficient with previous diffusion expressions. These results will illustrate the difficulties inherent to the previous coefficients while exhibiting the capability of the new anisotropic diffusion process to maintain edge locations while smoothing small scale features.

IV. Results and Conclusions

To display the effectiveness of the new morphological diffusion coefficient, simulations were conducted with three classes of the anisotropic diffusion coefficient. The first class was dependent solely on local gradient information and represented by the coefficient described by (3). The second and third classes employed scale-modified definitions for the gradient. The second class used a linear filter in performing the gradient calculation while the third class used a nonlinear morphological filter. These classes were represented by coefficients described by (4) and (5), respectively.

Realization of a discrete representation of the anisotropic diffusion equation utilized an approximation suggested in [6]. The iterative solution is given as

$$\mathbf{I}_{i,j,t+\Delta t} = \mathbf{I}_{i,j,t} + \Delta t\left(c_N\nabla_N + c_S\nabla_S + c_E\nabla_E + c_W\nabla_W\right), \tag{6}$$

where $\mathbf{I}_{i,j,t}$ is the image pixel value at location (i,j) for solution time t, $\nabla_N, \nabla_S, \nabla_E, \nabla_W$ are the image gradients (simple differences) in the north, south, east, and west directions respectively, c_N, c_S, c_E, c_W are the corresponding diffusion coefficients, and Δt is the solution time step.

Equivalent scale parameters for the linear and morphological filters in the scale aware diffusion coefficients were chosen to provide information removal of similar scale, and both were defined by satisfying conditions necessary for subsampling the filtered representations by a factor of three. The Gaussian kernel

used in the second coefficient class was defined to have a standard deviation of $6/\pi$, as suggested to satisfy Shannon's sampling theorem in [1]. Similarly, the morphological kernel used in the third coefficient class was defined to be a square structuring element of width five, as suggested to satisfy the Homotopy Preserving Critical Sampling Theorem in [3].

Producing a qualitative evaluation of the three processes, the anisotropic diffusion equation was applied to synthetic imagery corrupted by 40% salt and pepper noise. Results are shown in Figure 1. As claimed in the second section, the diffusion equation based solely on local gradient information is unable to remove impulsive noise, while both spatially enlarged coefficients are capable of smoothing these small, high contrast objects and maintaining large scale edges. Results for coefficient classes two and three are visually similar, although closer inspection will show that the third class, the nonlinear morphological method, provides a slight improvement in feature definition.

A second qualitative example of the three anisotropic diffusion processes was attained by applying the smoothing operations to the cameraman image. These results are similar to those achieved with the previous synthetic imagery, and they are presented in Figure 2. Again, the first coefficient class, using a traditional gradient calculation, is unable to remove fine detail, as evident by the existence of the small objects present on the ground. The second coefficient class, using a linear filter within its gradient calculation, removes these small features, but at the expense of introducing edge movement and feature drift. (Notice the excessive smoothing of the camera and the movement of the elbow.) The new morphological anisotropic diffusion algorithm is capable of overcoming both deficiencies, removing small objects while maintaining edge locality.

While qualitative comparison of the three methods of anisotropic diffusion begins to distinguish the smoothing properties of the morphological diffusion coefficient, a quantitative comparison of their edge detection accuracy displays the advantages of the new diffusion expression.

In determining the edge detection capabilities of the three variants of anisotropic diffusion, synthetic imagery was again corrupted by 40% salt and pepper noise. These images were then smoothed; and at each solution time, edges were identified and compared with known edge locations. Recognizing edges in the filtered imagery was accomplished with the use of a simple Sobel edge detector, well motivated by the smoothing properties of the anisotropic diffusion equation, and the threshold of the edge detector was defined to be equal to the gradient threshold of the diffusion coefficient, k.

Experimental comparison of edge detection performance was calculated using two quantitative metrics. The first, Pratt's edge quality measurement, is defined as

$$F = \frac{\sum_{i=1}^{I_A} \frac{1}{1+\alpha\left(\mathrm{d}(i)^2\right)}}{\max\{I_A, I_I\}} \tag{7}$$

where I_A is the number of edge points detected in the filtered image result, I_I is the number of edge points existing in the original, noise free imagery, $\mathrm{d}(i)$ is the Euclidean distance between an edge location in the original image and the nearest detected edge, and α is a scaling constant, set to the suggested value of 1/9 [7]. Perfect recovery of all edge information in the original image results in an edge quality measurement of one (F=1); poor edge localization lowers the value.

The second measurement contains a more tangible representation of the candidate filter performance and is defined to be the percentage of original edge points successfully identified by the edge detection process. Correctly recovering all edges in the initial image results in a 100% identification percentage, not detecting a feature at its original location lowers the identification measurement.

The results of the numerical experiment are presented in Figure 3. We see that the linear coefficient initially outperforms the other diffusion variants in the edge quality measurement, but produces the poorest identification percentage. As solution time increases, the introduction of edge localization errors by the linear filter becomes more evident and is displayed by the rapid decrease in matched features. Specifically, at solution time three, the linear coefficient is unable to correctly identify the location of a single edge. The morphological anisotropic diffusion method provides significant performance improvement, able to identify over 70% of the original edges and attain a solution quality measurement of .95.

V. References

[1] P.J. Burt, "Fast Filter Transforms for Image Processing," in Computer Graphics and Image Processing, vol.16, no.1, pp.20-51, 1981.

[2] F. Catté, P.-L. Lions, J.-M. Morel, and T. Coll, "Image selective smoothing and edge detection by nonlinear diffusion," SIAM J. Numerical Analysis, vol.29, no.1, pp.182-193, 1992.

[3] D. A. F. Florencio and R. W. Schafer, "Homotopy and Critical Morphological Sampling," *Proc. of SPIE Symposium on Visual Communications and Image Processing*, Chicago, September 1994.

[4] R. M. Haralick, S. R. Sternbeg, and X. Zhuang, "Image analysis using mathematical morphology," IEEE Trans. on PAMI, vol.9, no.4, pp. 532-550, 1987.

[5] J.J. Koenderink, "The structure of images," J. Biol. Cybern., vol.50, pp.363-370, 1984.

[6] P. Perona and J. Malik, "Scale-space and edge detection using anisotropic diffusion," IEEE Trans. on PAMI, vol.12, no.7, pp.629-639, 1990.

[7] W.K. Pratt, *Digital Image Processing*. New York: Wiley, pp. 495-501, 1978.

[8] J. Serra, *Image Analysis and Mathematical Morphology*, vol.2. New York: Academic Press, 1988.

[9] Y. You, W. Xu, A. Tannenbaum, and M. Kaveh, "Behavioral Analysis of Anisotropic Diffusion in Image Processing," IEEE Trans. on IP, vol.5, no.11, pp.1539-1553, 1996.

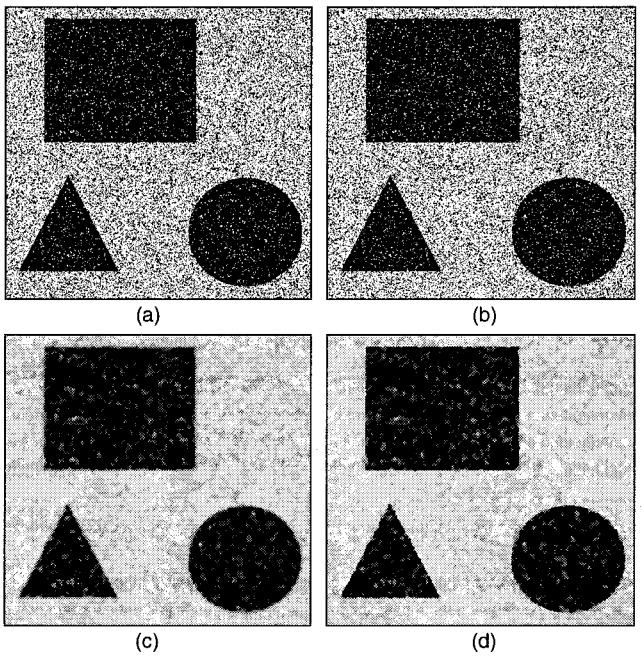

Figure 1. Three classes of anisotropic diffusion applied to synthetic imagery: (a) original image corrupted with 40% salt and pepper noise; (b) results obtained using (3); (c) results obtained using (4); (d) results obtained using morphological anisotropic diffusion (5). The gradient threshold, *k*, was 40 and the solution time was 3.

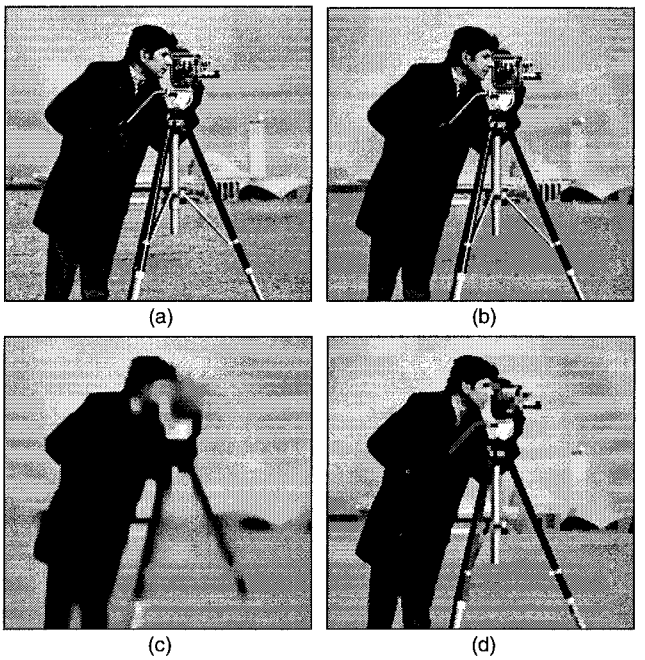

Figure 2. Three classes of anisotropic diffusion applied to the cameraman image: (a) original image; (b) results obtained using (3); (c) results obtained using (4); (d) results obtained using morphological anisotropic diffusion (5). The gradient threshold, *k*, was 10 and the solution time was 20.

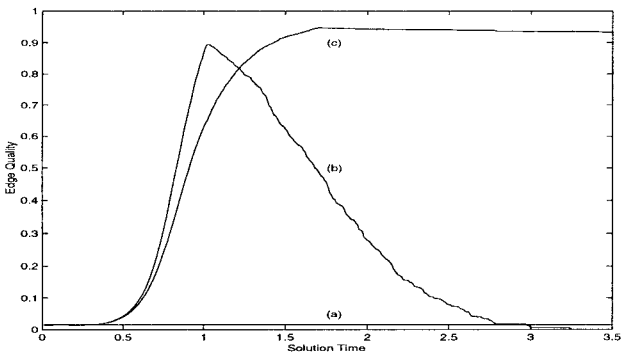

Figure 3a. Pratt's measurement of edge quality: (a) results obtained from (3); (b) results obtained using (4); (c) results obtained using morphological anisotropic diffusion (5). The gradient threshold, *k*, was 40.

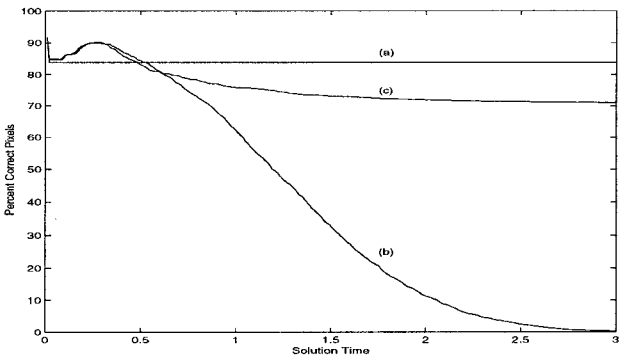

Figure 3b. Percentage of edges correctly identified: (a) results obtained from (3); (b) results obtained using (4); (c) results obtained using morphological anisotropic diffusion (5). The gradient threshold, *k*, was 40.